1 ***Chlamydomonas reinhardtii* exhibits stress memory in the accumulation of triacylglycerols induced**
2 **by nitrogen deprivation**

3 **Pawel Mikulski[1*], Javier Santos-Aberturas[2]**

4 1 Cell and Developmental Biology, John Innes Centre, Norwich, UK

5 2 Molecular Microbiology, John Innes Centre, Norwich, UK

6 * corresponding author

7

8 **Summary**

9 Stress memory is a phenomenon whereby exposure to initial stress event influences a response to
10 subsequent stress exposures. Studying stress memory is important to understand the cellular
11 behaviour in dynamic environment, especially nowadays, in times with growing environmental
12 instability. Stress memory has been characterized in vascular plants but its occurrence in non-vascular
13 plant species has been rarely investigated.

14 We hypothesized that stress memory occurs in non-vascular plants in relation to metabolic stress. We
15 sought to test it using accumulation of lipids (triacylglycerols) in model green alga *Chlamydomonas*
16 *reinhardtii* subjected to nitrogen deprivation stress as a model system.

17 Here, we established stress memory protocol on *C. reinhardtii* cells. Using a blend of microscopy and
18 gas chromatography methods, we showed that the cells exposed to recurrent stress show differential
19 accumulation of triacylglycerols on the quantitative level without qualitative changes in lipid
20 composition, comparing to single stress controls.

21 Overall, our results suggest that metabolic stress memory does occur in non-vascular plant *C.*
22 *reinhardtii* and provides a starting point to characterize metabolic stress memory mechanism. Due to
23 the commercial potential of algae, our findings are relevant for basic science, as well as industrial
24 production of algae-derived compounds.

25

26 **Keywords:** algae, triacylglycerols, stress memory, biofuel, epigenetics, Chlamydomonas

27

28 **Introduction**

29 Stress memory is a phenomenon whereby exposure to initial stress event influences a response to
30 subsequent stress exposures. Its importance is highlighted especially nowadays, in times with growing
31 environmental instability (IPCC, 2018). Stress memory has been characterized in vascular plants
32 (Mozgova *et al.*, 2019), where it is related to, i.e., response to drought (Ding *et al.*, 2012) or
33 temperature (Brzezinka *et al.*, 2016). However, the occurrence of stress memory has been only rarely
34 reported in non-vascular plants (Widiez *et al.*, 2014; Korkaric *et al.*, 2015), and still remains a largely
35 unexplored niche.

36   Unicellular algae form a powerful biotechnological warehouse for production of chemical compounds.
37   Triacylglycerols (TAGs) are lipids that can be used as the precursors in biodiesel production for
38   academic and industrial research. Model green alga, *Chlamydomonas reinhardtii*, accumulates TAGs
39   in stress conditions such as nitrogen deprivation (Park *et al.*, 2015). TAGs accumulation is reversible
40   (Roustan *et al.*, 2017) and chromatin-based (Ngan *et al.*, 2015), features that make this process a
41   potential subject for stress priming.

42   How TAGs' accumulation behaves in *C. reinhardtii* subjected to multiple nitrogen deprivation events
43   and whether the species exhibits metabolic stress priming has not been investigated. We
44   hypothesized that stress memory occurs in the accumulation of TAGs in *C. reinhardtii* subjected to
45   nitrogen deprivation. Here, we established a stress priming growth protocol in *C. reinhardtii*. Using a
46   blend of microscopy and gas chromatography, we showed that algal cells exposed to recurrent stress
47   show differential accumulation of triacylglycerols on the quantitative level without qualitative changes
48   in lipid composition, comparing to single stress controls.

49   This work provides a proof-of-principle evidence that metabolic stress memory does occur in non-
50   vascular plant *C. reinhardtii* and opens a new avenue to understand the mechanisms behind stress
51   memory and cellular response to the fluctuating environment. Due to commercial potential of algae
52   and usage of stress-induced processes for production of biologics, this work offers a contribution to
53   academic and industrial researchers.

54

Material and methods

Growth conditions and growth medium

57   Wildtype *C. reinhardtii* strain 137c was grown in liquid cultures on TAP medium with agitation at 180
58   rpm as described previously (Ngan *et al.*, 2015). For nitrogen depletion, TAP medium without nitrogen
59   source was used as described in (Ngan *et al.*, 2015). The cells were washed twice with nitrogen-
60   depleted medium before media change during stress treatment. Alga cultures were kept in growth
61   cabinets (Sanyo-MLR-352-PE) set for 25°C and supplied with LED fluorescent lights (Newlec,
62   NL/18/LED/T8/4/865 & 840).

Fixation & Nile Red staining

64   We performed TAGs' staining with Nile Red dye on fixed cells. We used 3% (v/v) formaldehyde (FA)
65   on 1 ml culture aliquots, incubated for 20 min on ice, spun at 3000 rpm for 5 min and washed twice
66   with phosphate saline buffer (PBS). Final cell pellet was resuspended in 20-50 µL PBS based on
67   estimation from OD600. 6-7 µL of final solution was spread onto microscopy slides, air dried and
68   refrigerated until staining. Staining was done with 5 µg/mL in 0.1 % acetone for 15 min in dark.

Microscopy and image analysis

70   Image acquisition was performed in two channels: Ex488/Em520-600 and Ex633/Em635-700 (Ex =
71   excitation, Em = emission), where former corresponds to specific Nile Red signal and the latter to cell
72   autofluorescence. For intensity quantifications, Ex488/Em520-600 channel was used to avoid a
73   crosstalk with autofluorescence channel. For Z-stacks, we used a step size (z-distance between slices)
74   of 0.55-0.59 µm and line averaging at 2. Following parameters for image acquisition were used: scan
75   speed at 400 Hz, pinhole size at 1 Airy unit (AU) and laser power at 16%. Image analysis was performed

76 in Fiji/ImageJ. Nile Red intensity quantification was done in 3 biological replicates per harvesting point
77 and sample type. We quantified intensity from 154-300 cells per sample. Statistical analysis was done
78 using Student's T-test.

79 **Total lipid extraction**

80 From 100 ml culture in each time point (ZT), we harvested 2ml aliquot and centrifuged it (4000 rpm,
81 10 min) in 20 ml glass vials. The supernatant was discarded and cell pellet equalized between the
82 samples. The pellet was mixed with 1 mL of chloroform/methanol 2:1 by vigorous vortexing (2500
83 rpm, 30 min) and then centrifuged (4500 rpm, 10 min). 500 µL of resuspended pellet was transferred
84 to clean 2 ml glass vial, vortexed (2500 rpm, 20 min) with 200 µL of LC-MS-grade water to extract polar
85 molecules and left for gravity phase separation. The lower, organic layer containing lipids was
86 transferred to clean 2 ml GC-MS glass vial and evaporated to dryness in a GeneVac evaporator, being
87 finally ready for analysis by GC-MS.

88 **GC-MS**

89 GC-MS analyses were performed on an Agilent 7890B GC system coupled to an Agilent 5977A Mass
90 Selective Detector, using a Phenomenex Zebron ZB5-HT Inferno (35m x 250 µm x 0.1 µm). The TAGs
91 and other fatty acid esters contained in the dry samples were resuspended and derivatized with
92 methanol into fatty acid methyl esters via alkali catalysis in an automated fashion before the injection
93 of each sample. The injector and interface were operated at 275 °C and 230 °C, respectively, and the
94 oven heated from 50 °C to 260 °C at a rate of 7 °C min^{-1} and then isothermally held for 5 minutes. The
95 total run time for each sample was 37 min. Helium was used as carrier gas, with a flow of 2 ml min^{-1}.
96 1 µL of sample was injected in splitless mode. The MS was operated in scan mode (50-500 Da), with
97 an ionization energy of 70 eV.

98

99 **Results**

100 **Establishment of stress memory growth setup**

101 As a first step, we sought to establish stress memory growth protocol for *C. reinhardtii*. We optimized
102 light intensity conditions (Fig.S1a) and tested culture growth in medium depleted of nitrogen source
103 or in default TAP medium with standard nitrogen source concentration (Ngan *et al.*, 2015). As
104 expected, our test showed substantial doubling and increased OD600 for cultures grown in default
105 medium, but not in the nitrogen-depleted samples (Fig.S1b).

106 Data published previously suggests that lipid accumulation in stressed *C. reinhardtii* cells reaches
107 substantial levels already after 2 day-long growth under nitrogen depletion without lethal effect in the
108 culture (Ngan *et al.*, 2015). Therefore, we designed stress priming setup, allocating 2 days for stress
109 treatment and 2 days for the recovery period (Fig.1a). We set samples to be treated with two nitrogen
110 depletion events (stress primed) or single stress event (control), harvesting aliquots for further
111 analyses at timepoints (*zeitgeber*): ZT2 and ZT4, as indicated on the scheme (Fig.1a). We used 3
112 biological replicates for each timepoint in nitrogen-deprived and nitrogen-control samples and used
113 harvested aliquots for microscopy or gas chromatography coupled with mass spectrometry (GC-
114 MS/MS) (Fig.1b). To exclude the possibility that 1st nitrogen depletion event interferes with a readout
115 from 2nd nitrogen depletion and ensure constant cell growth, we washed cultures with TAP-N

116   (nitrogen depleted medium) before each stress event and split the cells 1:1 directly after 1st stress
117   (after ZT2) and after recovery window - directly before 2nd stress (before ZT4). Our OD600
118   measurements suggested that the cells were actively dividing after nitrogen depletion events (Fig.1c).

119   **Optimization of TAG staining and image analysis workflow**

120   Using previously harvested aliquots at indicated timepoints, we sought to measure TAGs accumulation
121   through histochemistry, microscopy and image analysis. Firstly, we performed chemical fixation of
122   cells and their Nile Red staining of TAGs (see methods). Nile Red is an efficient TAG marker and its
123   fluorescence was reported to be tightly correlated with TAG concentration in *C. reinhardtii* (Johnson
124   *et al.*, 2017). Afterwards, we optimized confocal microscopy conditions (see methods) to separate Nile
125   Red signal from cellular autofluorescence and acquired Z-stacks of prepared specimens to capture Nile
126   Red signal in 3D. We observed only background autofluorescence in negative microscopy controls
127   (mock-stained nitrogen-depleted (N-) or Nile Red-stained nitrogen-control (N+) samples) without
128   specific Nile Red signal (Fig.2a). In contrast, Nile Red-stained nitrogen-depleted specimen showed
129   TAGs' accumulation in lipid bodies, as reported previously (Wang *et al.*, 2009), and selective Nile Red
130   signal (Fig.2a), which confirmed specificity of staining and microscopy workflow.

131   To properly quantify Nile Red-stained TAG accumulation, we established a workflow for image
132   analysis. Firstly, we converted Z-stack to single images by slice summing in Z-projection. Afterwards,
133   we segmented cells with minimum error threshold to create masks used as regions-of-interest (ROIs)
134   outlining cell borders. Finally, we quantified mean fluorescence intensity in grey value inside ROIs as
135   a way to measure Nile Red-stained TAG intensity. The examples of different workflow stages are
136   present in Fig. 2b.

137   **TAG intensity quantification**

138   Following measurement of a raw Nile Red-stained TAGs' fluorescence intensity, we normalized
139   technical differences between the images. To this end, we quantified background fluorescence
140   outside the cells on the image and subtracted its value from the specific Nile Red signal from within
141   the cells. We used normalized intensity measurements compare stress-primed sample at ZT4 (2nd
142   stress exposure) with its controls: stress-memory samples at ZT2 (1st stress exposure, ZT2 N --) and
143   single-stressed samples at ZT4 (ZT4 N +-). To ensure statistical power of the analysis, each sample had
144   3 biological replicates and the intensity measurements in each biological replicate was done on 154-
145   300 cells.

146   As a result, we observed a clear and significant difference between stress-primed samples and single-
147   stressed controls. Stress-primed samples showed downregulation of TAGs' fluorescence intensity
148   (Fig.3a, b), suggesting a differential response to recurrent nitrogen deprivation conditions and a
149   memory effect of previously encountered stress. We do not envisage that an observed effect at ZT4
150   (2nd stress) is a technical bleed-through from ZT2 (1st stress), since cells has been split twice before ZT4
151   and the cultures were actively dividing throughout the experiment (Fig.1c). In turn, this observation
152   in such experimental setup suggests a memory effect that is heritable over cell division and potentially
153   of epigenetic nature.

154   **TAG profiling using GC-MS/MS**

155   To qualitatively assess the lipid composition of the accumulated TAGs and complement the confocal
156   microscopy measurements, we performed a gas chromatography mass spectrometry (GC-MS)

157   lipidomic analysis. We extracted lipids from stress-primed cultures (ZT4 N-/-) and single-stressed
158   control harvested at the same time (ZT4 N+/-). The extracted lipids underwent transesterification to
159   generate volatile fatty acid methyl esters (see methods), which were subsequently analysed by GC-
160   MS, along with standard fatty acid libraries.

161   Our results reveal that the qualitative profile of lipid types did not show substantial differences
162   between stress-primed samples and single-stressed controls (Fig.4), despite different lipid
163   accumulation observed through histochemistry. This observation suggests that quantitative stress
164   priming response in TAGs accumulation does not come with qualitative change in lipid composition.

165

Discussion

167   In summary, we observed a differential TAG accumulation caused by stress memory in
168   Chlamydomonas cells. Cells subjected to two rounds of nitrogen depletion events show attenuated
169   TAG accumulation, compared to single-stressed counterparts. Interestingly, this change was observed
170   on quantitative level, as judged from histochemical measurements, but not in qualitative fashion –
171   stress-memory samples do not exhibit substantial differences in the abundance of lipid subtypes,
172   comparing to the controls. TAGs quantitative downregulation in stress-memory samples indicates that
173   cells exhibit attenuated nitrogen deprivation response based on the previous stress exposure or
174   respond to further stress events with pathways antagonistic to TAGs' accumulation. Given the ongoing
175   growth of the culture throughout the experiment, we envisage that observed response in stress-
176   memory samples is potentially of epigenetic nature. Future steps should aim to elucidate the
177   mechanism of stress memory and identify its causal factors.

178   In conclusion, our results highlight that metabolic stress memory of nitrogen depletion exists in model
179   green alga and suggests that metabolic stress memory mechanisms could be widely conserved in non-
180   vascular plants.

181

Acknowledgements

Author contribution

190   PM and JSA designed the research and performed culture harvesting. PM performed TAG staining,
191   microscopy, image analysis and intensity quantification. JSA performed lipid extraction, gas
192   chromatography and spectrometry peak analyses. PM, together with JSA, wrote the manuscript.

Conflict of interest

194   The authors declare no conflict of interest.

References

Brzezinka K, Altmann S, Czesnick H, Nicolas P, Gorka M, Benke E, Kabelitz T, Jähne F, Graf A, Kappel C, *et al.* **2016**. Arabidopsis FORGETTER1 mediates stress-induced chromatin memory through nucleosome remodeling. *eLife*.

Ding Y, Fromm M, Avramova Z. **2012**. Multiple exposures to drought 'train' transcriptional responses in Arabidopsis. *Nature Communications*.

IPCC. **2018**. *IPCC Global Warming of 1.5°C Summary For Policymakers*.

Johnson ZI, Bidigare RR, Blinebry SK, Brown SL, Cullen JJ, Loftus SE, Redalje DG, Swink C, Van Mooy BAS. **2017**. Screening for Lipids from Marine Microalgae Using Nile Red. In: Consequences of Microbial Interactions with Hydrocarbons, Oils, and Lipids: Production of Fuels and Chemicals.

Korkaric M, Xiao M, Behra R, Eggen RIL. **2015**. Acclimation of Chlamydomonas reinhardtii to ultraviolet radiation and its impact on chemical toxicity. *Aquatic Toxicology*.

Mozgova I, Mikulski P, Pecinka A, Farrona S. **2019**. Epigenetic mechanisms of abiotic stress response and memory in plants. In: Epigenetics in Plants of Agronomic Importance: Fundamentals and Applications: Transcriptional Regulation and Chromatin Remodelling in Plants: Second Edition.

Ngan CY, Wong CH, Choi C, Yoshinaga Y, Louie K, Jia J, Chen C, Bowen B, Cheng H, Leonelli L, *et al.* **2015**. Lineage-specific chromatin signatures reveal a regulator of lipid metabolism in microalgae. *Nature Plants*.

Park JJ, Wang H, Gargouri M, Deshpande RR, Skepper JN, Holguin FO, Juergens MT, Shachar-Hill Y, Hicks LM, Gang DR. **2015**. The response of Chlamydomonas reinhardtii to nitrogen deprivation: A systems biology analysis. *Plant Journal*.

Roustan V, Bakhtiari S, Roustan PJ, Weckwerth W. **2017**. Quantitative in vivo phosphoproteomics reveals reversible signaling processes during nitrogen starvation and recovery in the biofuel model organism Chlamydomonas reinhardtii. *Biotechnology for Biofuels*.

Wang ZT, Ullrich N, Joo S, Waffenschmidt S, Goodenough U. **2009**. Algal lipid bodies: Stress induction, purification, and biochemical characterization in wild-type and starchless chlamydomonas reinhardtit. *Eukaryotic Cell*.

Widiez T, Symeonidi A, Luo C, Lam E, Lawton M, Rensing SA. **2014**. The chromatin landscape of the moss Physcomitrella patens and its dynamics during development and drought stress. *Plant Journal*.

Figure captions

Fig.1 Stress memory growth schematic and cell growth. a. Stress memory growth scheme. ZT (*zeitgaber*) indicate harvesting timepoints for TAG measurements. N+ and N- labels correspond to nitrogen-control and nitrogen-depleted growth conditions., respectively. **b.** Post-harvesting workflow schematic **c.** Growth measurements (OD600) of cells in stress memory experiment. Error bars correspond to standard error from 3 biological replicates (separate flasks).

231 **Fig.2 TAG staining and microscopy workflow. a.** Exemplar images for Nile Red- and mock-stained
232 samples. N- label corresponds to nitrogen-depleted samples, whereas N+ to control with standard
233 nitrogen source concentration. The arrows correspond to examples of lipid bodies specifically stained
234 by Nile Red. **b.** Image analysis workflow: A) Z-projection for Nile Red-specific channel; B) cell
235 segmentation with pixel intensity thresholding; C) cell annotation on binary image D) cell annotation
236 on original image for intensity quantification. Scale bar corresponds to 5 μm.

237 **Fig.3 Imaging of TAG accumulation a.** Representative images of TAG-stained cells from stress-memory
238 samples (N --) and single-stressed controls (N +- and N – at 1st nitrogen depletion). Scale bar
239 corresponds to 10 μm **b.** Nile Red intensity quantification as a proxy for TAG accumulation
240 measurements. Error bars correspond to SEM from 3 biological replicates and statistics were
241 calculated using Student's t-test in comparison: ZT2 N– to ZTN– and ZT4 N+- to ZT4 N--.

242 **Fig.3 TAG profiling through GC-MS/MS.** GC-MS TAG profiling. Chromatograms depict retention peaks
243 of single-stressed ZT4 N+- and stress-primed ZT4 N– samples, each in 3 biological replicates as
244 indicated in the numbers on the side labels. Two top bars correspond to GC-MS/MS lipid standards.
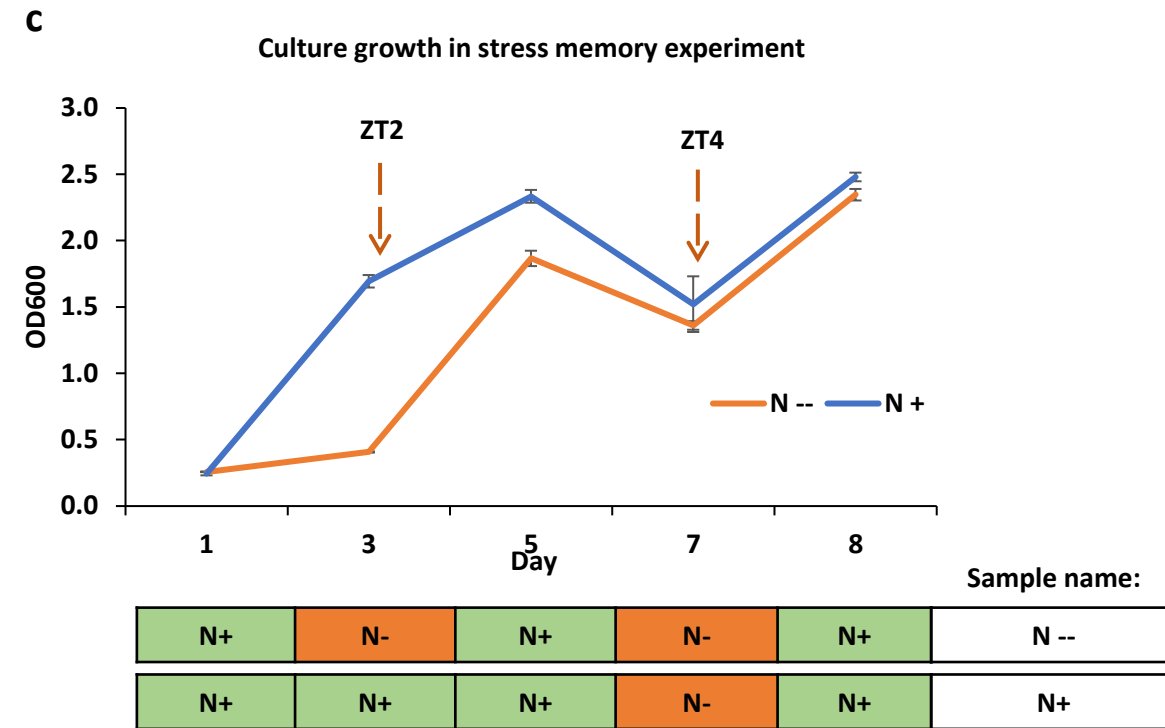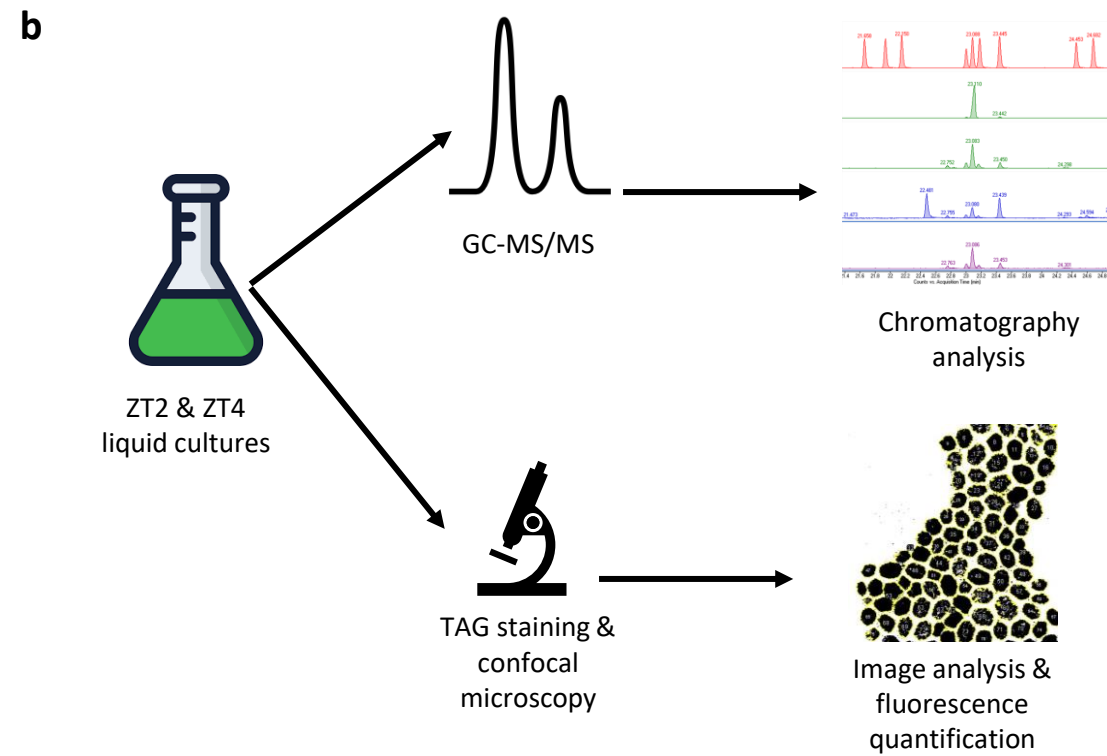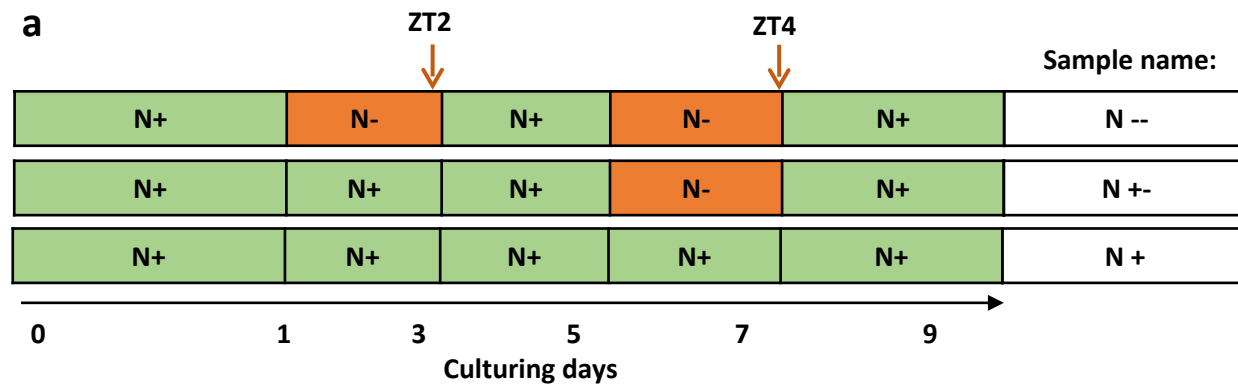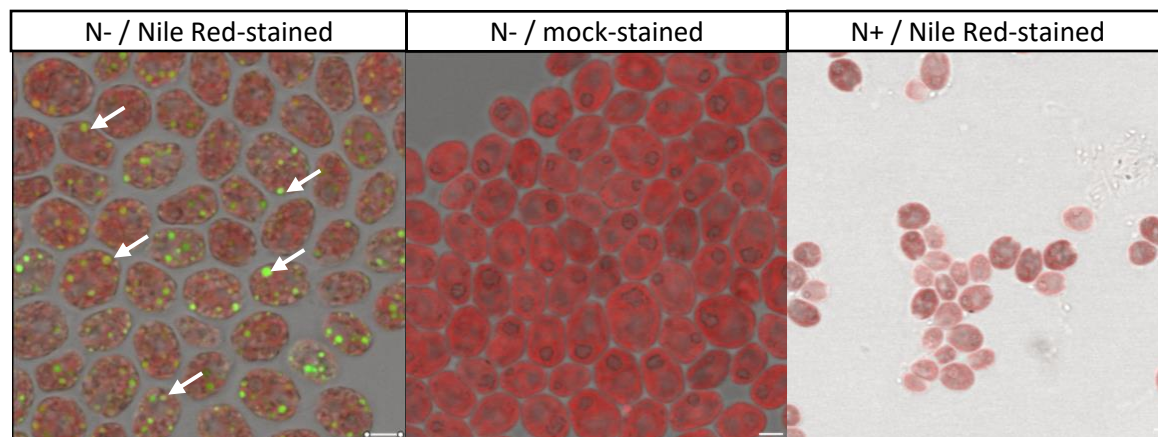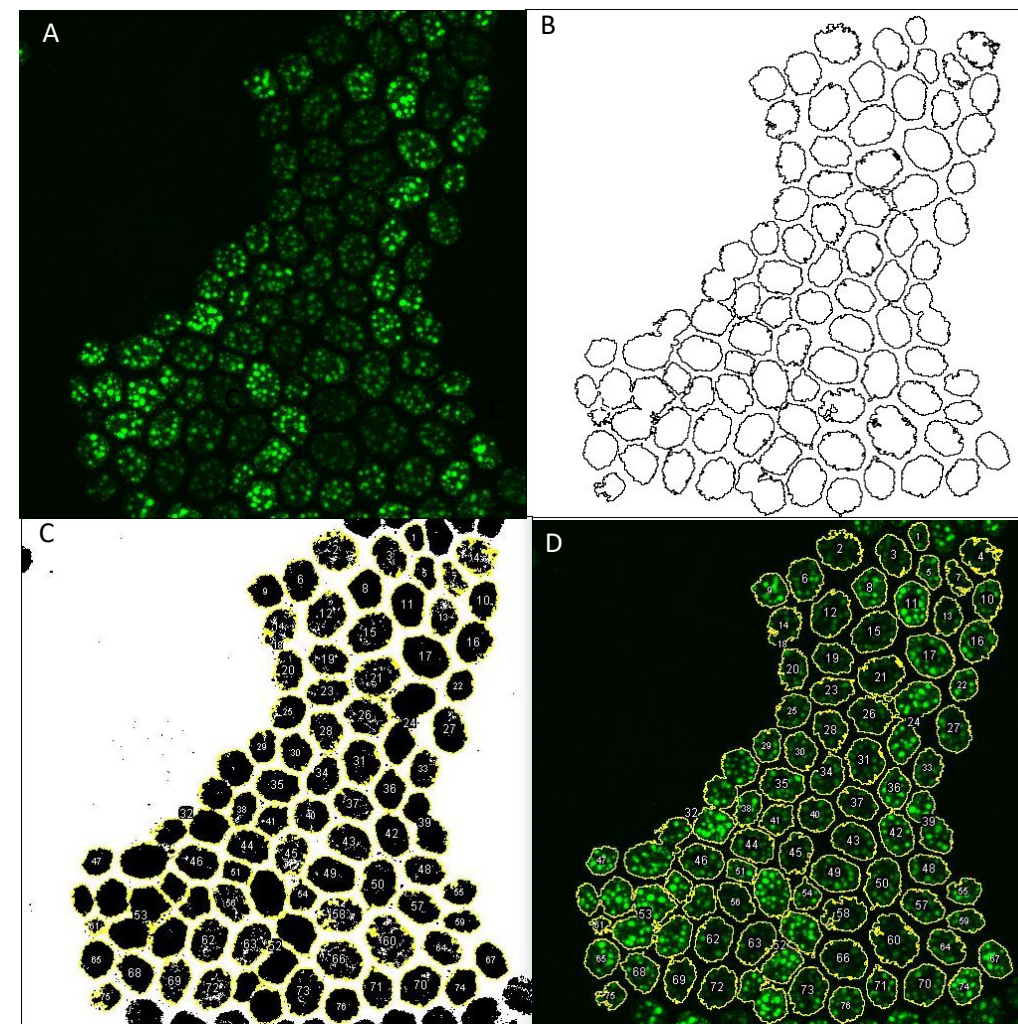
245

246

Fig.1 Stress memory growth schematic and cell growth. a. Stress memory growth scheme. ZT (*zeitgaber*) indicate harvesting timepoints for TAG measurements. N+ and N- labels correspond to nitrogen-control and nitrogen-depleted growth conditions., respectively. **b.** Post-harvesting workflow schematic **c.** Growth measurements (OD600) of cells in stress memory experiment. Error bars correspond to standard error from 3 biological replicates (separate flasks).

Fig.2 TAG staining and microscopy workflow. a. Exemplar images for Nile Red- and mock-stained samples. N- label corresponds to nitrogen-depleted samples, whereas N+ to control with standard nitrogen source concentration. The arrows correspond to examples of lipid bodies specifically stained by Nile Red. **b.** Image analysis workflow: A) Z-projection for Nile Red-specific channel; B) cell segmentation with pixel intensity thresholding; C) cell annotation on binary image D) cell annotation on original image for intensity quantification. Scale bar corresponds to 5 μm.
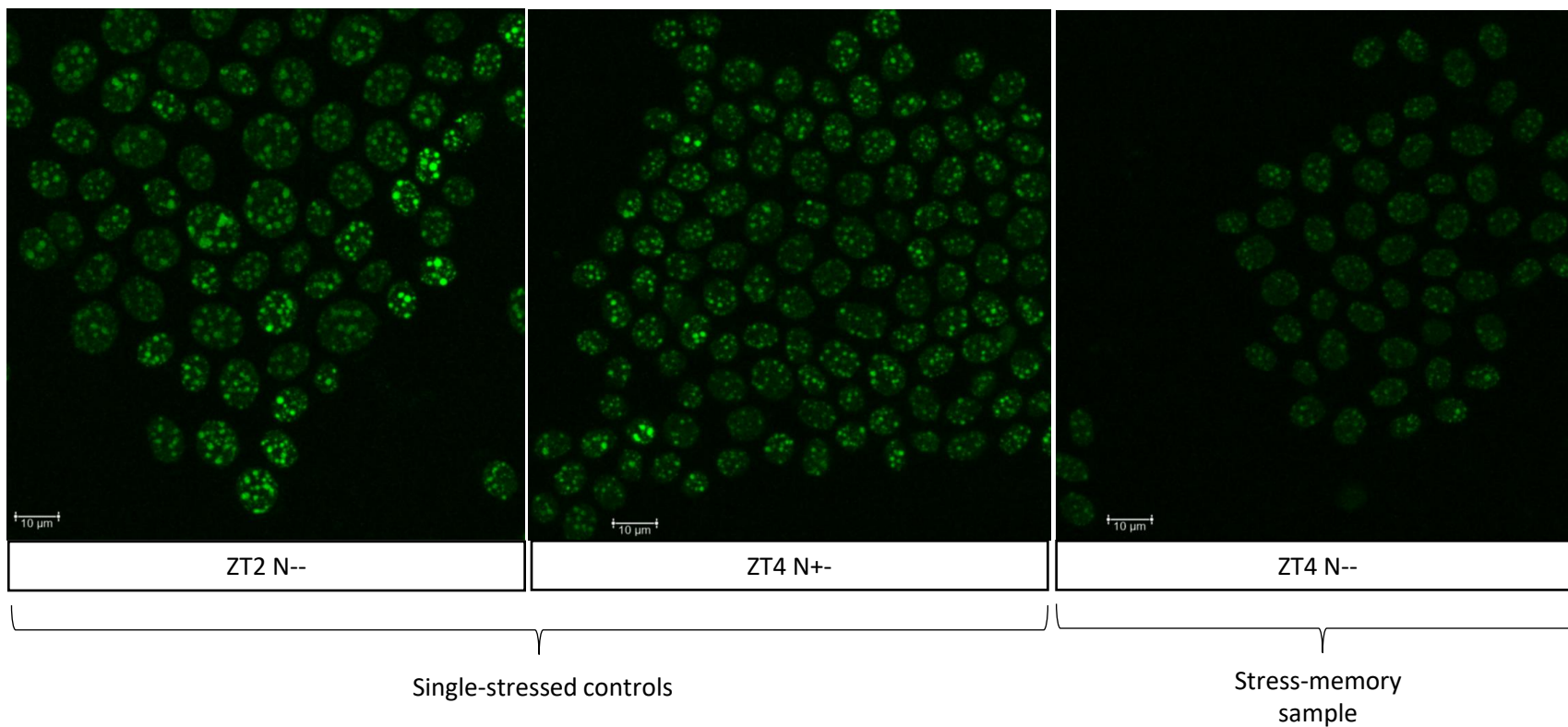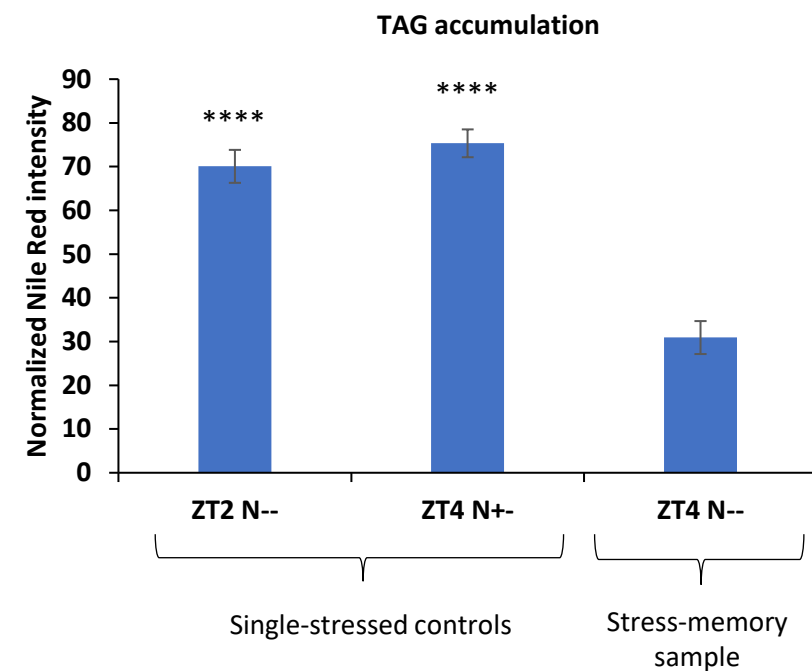
Fig.3 Imaging of TAG accumulation a. Representative images of TAG-stained cells from stress-memory samples (N --) and single-stressed controls (N +- and N – at 1st nitrogen depletion). The images correspond to maximum projection of individual Z-stack from respective sample. Scale bar is set to 10 μm. **b.** Nile Red intensity quantification as a proxy for TAG accumulation measurements. Error bars correspond to SEM from 3 biological replicates and statistics were calculated using Student's t-test in comparison: ZT2 N– to ZTN– and ZT4 N+- to ZT4 N--.
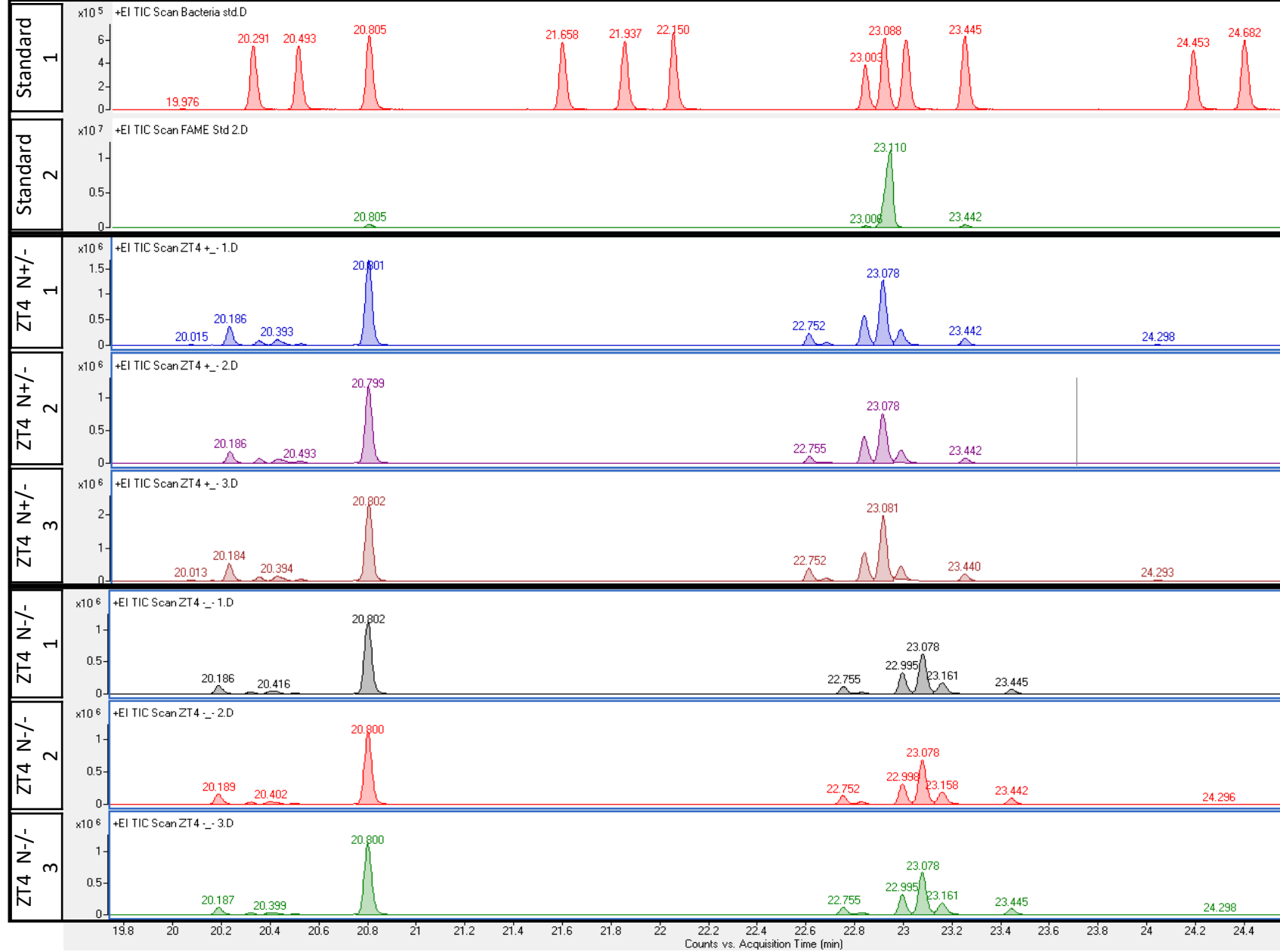
Fig.3 TAG profiling through GC-MS/MS. GC-MS TAG profiling. Chromatograms depict retention peaks of single-stressed ZT4 N+- and stress-primed ZT4 N– samples, each in 3 biological replicates as indicated in the numbers on the side labels. Two top bars correspond to GC-MS/MS lipid standards.